ANALYSIS OF TRANSONIC FLOW PAST CUSPED AIRFOIL TRAILING EDGE

Jiří Stodůlka*, Pavel Šafařík

CTU in Prague, Faculty of Mechanical Engineering, Department of Fluid Mechanics and Termodynamics, Technická 4, 166 07 Prague 6, Czech Republic

* corresponding author: Jiri.Stodulka@fs.cvut.cz

ABSTRACT. In order to verify the limits of theoretical design methods, a transonic flow past two designed cusped airfoils is numerically solved and studied. The achieved results are compared with the theoretical predictions and then analyzed in terms of flow behavior and oblique shocks formation using known classical gas dynamics relations. The regions around the sharp trailing edges are studied in detail and parameters of shock waves are solved and compared using the classical shock polar approach and verified by reduction parameters for symmetric configurations.

KEYWORDS: oblique shock; shock polar; trailing edge; cusped airfoil; transonic flow; CFD.

1. INTRODUCTION

To this day, transonic flow has represented a very challenging topic. Although modern CFD is very powerful, it is good to keep classical methods in mind in order to verify the data obtained from numerical simulations, as nicely reminded in [1]. For a demonstration of such analyses, some cases from the pre-computational era are still relevant and can be used as perfect examples, thanks to their known analytical solutions and limits. One such example of a cusped airfoil pointed into sonic free stream that has been studied in depth using modern CFD tools, and which is exactly described by near sonic theory [2] can be found in reference [3]. Even though a good correspondence was found between design theory and the numerics, there are still bounds or limits beyond which the results are invalid and therefore questionable. To confirm the observed behavior, classical gas dynamics methods can be used to evaluate the character of the flow field. More specifically, they can be used to evaluate the parameters of oblique shock waves formed at the trailing edge and to see if any deviations from standard behavior can appear, especially near the limits of the transonic design methods.

2. THEORY AND DESIGN OF TRANSONIC CUSPED AIRFOILS

The mathematical methods solving transonic flow field are based on potential equations. To avoid nonlinearity of the basic system, the solution is transformed into a modified hodograph plane replacing the physical coordinates x, y with the new, azimuthal angle ϑ and with the Prandtl-Mayer angle υ. Concentrating only on flow with small perturbations to sonic flow simplifies the system enough to get an exact solution for both subsonic field, using conformal mapping methods, and supersonic field, using the method of characteristics. Finding analytical solutions to the above hodograph relations, described in [2], allows us to derive the formulae defining the shape, flow conditions and pressure coefficient for cusped airfoils in a uniform sonic flow $M = 1$. The solution of such airfoils is described in Fig. 1 and a schematic view of a cusp with all the defined parameters is shown in Fig. 2 [2]

The solution in real plane is on the left in Fig. 1 The modified hodograph plane on the right with axis T corresponds to the flow angle and S a function of the Mach number or the Prandtl-Meyer angle. The sharp leading edge (point A) cuts through the sonic flow at a certain angle. Then, due to smooth acceleration of the transonic flow from sub- to supersonic past the airfoil, crossed sonic lines appear (B, E). Up to this point, quasi-conformal mapping is used, and from here the solution is switched to characteristic mapping. The neutral characteristics (C, F) appear and the flow is still accelerating smoothly up to the trailing edge where two oblique shocks are formed (D, G).

The previous solution results in the cusp shape described by two parameters: the thickness parameter τ, defined as the thickness to chord ratio, and the camber parameter ω, defined as the camber to chord ratio. The solution is exact for $\tau \to 0$ and practically valid for slender airfoils with $\tau \leq 0.5$. The case with camber to chord ratio $\omega = 0$ is symmetrical, and also known as "Guderley's cusp". The range of validity for cambered airfoils is given by $\omega/\tau \leq 0.5$.

The camber/thickness parameter which is afterwards used to generate the geometry and the flow description is given by

$$P\left(\frac{\omega}{\tau}\right) = 2^{13/2} \cdot 3^{3/2} \\ \cdot 5^{-7/2}\frac{\omega}{\tau}\left(1 + 2^{12} \cdot 3 \cdot 5^{-6}\left(\frac{\omega}{\tau}\right)^2\right)^{-1/2}. \quad (1)$$

When the cusp is cambered, it is pointing into the flow and it is smoothly passed by the stream, so the
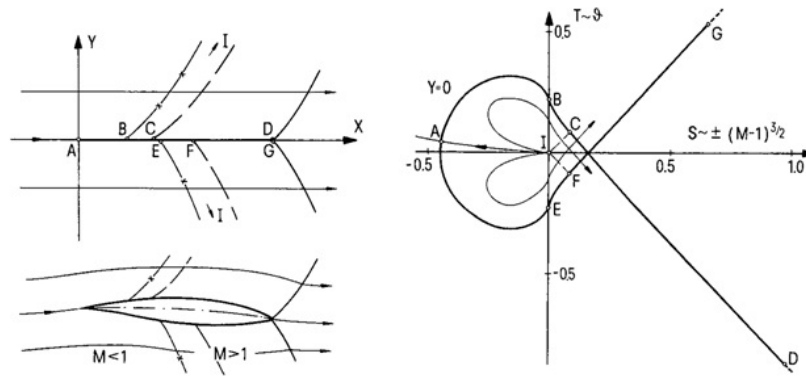
FIGURE 1. Cusp solution in the real and the rheograph plane [2].
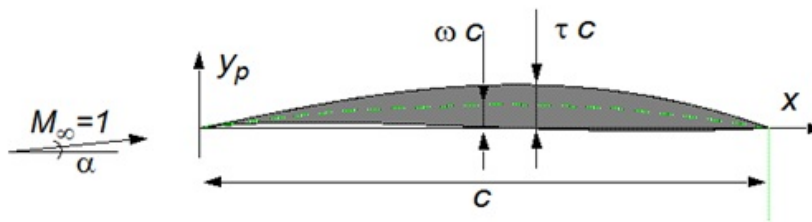

FIGURE 2. The cusp solution and parameters [3].

flow is not forced to change its direction around the sharp leading edge. The angle of attack is then

$$\alpha = \tau \cdot 2^{-9/2} \cdot 3^{-1/2} \\ \cdot 5^{5/2} P \frac{1 - 2^{-1} \cdot 3^{-4} \cdot 5 \cdot 13 P^2}{(1 - 2^{-1} \cdot 3^{-2} \cdot 5 P^2)^{3/2}}. \quad (2)$$

The geometry vertex data for the family of cambered airfoils are given by

$$y_p(X) = \tau \cdot X(1 - X) \\ \left(2^2 \frac{\omega}{\tau} \pm 2^{-2} \cdot 3^{-3/2} \cdot 5^{5/2} \cdot X^{1/2} \right). \quad (3)$$

and finally the pressure coefficient

$$c_p = \frac{(5^2 \cdot \tau)^{2/3}}{(2^2 \cdot 3(\kappa + 1))^{1/3}} \left(\frac{1 - 2^{-2} \cdot 3^{-2} \cdot 5 P^2}{1 - 2^{-1} \cdot 3^{-2} \cdot 5 P^2} \right. \\ \left. - 2^{-1} \cdot 5X \mp \frac{2^{-1/2} \cdot 3^{-1} \cdot 5P \cdot X^{1/2}}{(1 - 2^{-1} \cdot 3^{-2} \cdot 5 P^2)^{-1/2}} \right), \quad (4)$$

where κ is specific heat ratio.

Knowing this, we have a complete analytical solution of the problem of sharp cusped airfoils in a sonic free stream.

3. NUMERICAL SIMULATIONS

For numerical simulations, the two following variants were chosen: Case I with parameters somewhere in the middle of the exact solution bounds, $\tau = 0.05$ and $\omega/\tau = 0.02$ (Fig. 3a), and Case II at the limit of theoretical solution validity, with thickness to chord ratio $\tau = 0.1$ and parameter $\omega/\tau = 0.5$ (Fig. 3b). Case II is very interesting, because it is on the limit of validity, where the theory predicts a questionable solution
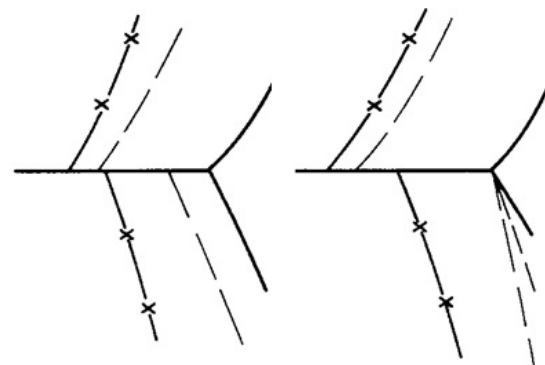

FIGURE 3. Predicted flow behavior.

around the lower side of the profile and around the trailing edge.

For the numerical simulation of the flow the inviscid Euler model dealing with ideal gas implemented in the ANSYS Fluent commercial CFD software was used. This simple model was chosen to be as comparable with the exact solution based on potential flow theory as possible. Some real gas applications to the transonic flow can be found, for instance in [4]. The AUSM numerical flux scheme was used on a structured quad mesh with the pressure far-field boundary condition that guarantees the sonic free stream. A detailed description of the simulation itself, the model, solver settings and boundary conditions is presented in [3]. The results describing the flow field behavior, shaded by contours of the Mach number for both variants are shown in Figs. 3.2 and 3.3.
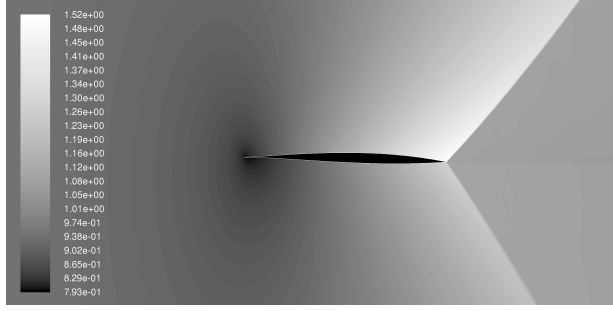
FIGURE 4. Contours of the Mach number, Case I, $\tau = 0.05$ and $\omega/\tau = 0.02$.
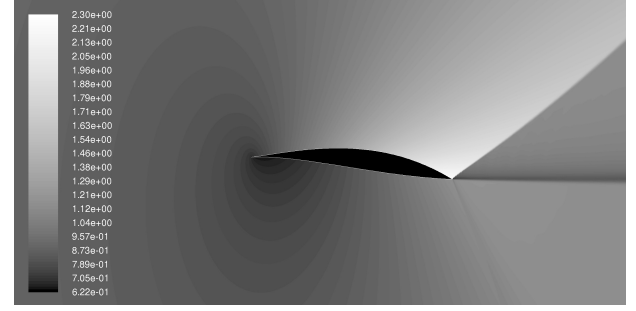

FIGURE 5. Contours of the Mach number, Case II, $\tau = 0.1$ and $\omega/\tau = 0.5$.

	Case I	Case II
M_1	1.51	2.29
M_2	1.27	1.15
δ_{TE}	15.1°	28.8°

TABLE 1. Gas dynamics analysis input data.

The results confirm the behavior of the flow expected from the theory. No shocks appear anywhere near the leading edge and the flow velocities are locally subsonic here. The flow is then smoothly accelerated along the profile to supersonic values. The supersonic region is subsequently closed by oblique shocks starting from the trailing edge. However, the differences between the variants are obvious. The first one (Fig. 4), a thin and slightly cambered case, forms two shocks with different strengths, while the second (Fig. 5), a thicker and cambered limit variant, produces higher Mach numbers and only one oblique shock on the upper side. On the lower side of the profile, the flow is not accelerated enough and no shock is visible here. Instead, there is a slip line recognizable behind the profile.

The situation around the trailing edge of the second variant especially encourages for further investigation, because as mentioned, it is the limit case, and so the theory cannot give us an absolutely exact solution here and all the CFD results ought to be validated before pronounced as relevant.

4. CLASSICAL GAS DYNAMICS ANALYSIS

The following physical model of supersonic flows interaction on a sharp trailing edge, depicted in Fig. 3, is formulated for the evaluation of oblique shock parameters. Shock wave a is a shock wave of the first family (a left-running shock wave) and shock wave b is a shock wave of the second family (a right running shock wave). The total pressures are equal:

$$p_{01} = p_{02}. \tag{5}$$

The basic conditions on the discontinuity d downstream of the sharp trailing edge are equality of static pressures

$$p_3 = p_4 \tag{6}$$

and equality of azimuthal flow angles

$$\vartheta_3 = \vartheta_4. \tag{7}$$

For the solution of the flow conditions, the shock polar diagrams are used. These diagrams give a family of possible solutions in terms of pressure ratio to turning angle dependencies for given values of Mach numbers M and angles of shock waves to incoming flow β as a parameter. The pressure ratio on the shock wave a is given by the following formula:

$$\frac{p_3}{p_1} = \frac{\kappa - 1}{\kappa + 1}\left(\frac{2\kappa}{\kappa - 1}M_1^2 \sin^2 \beta_a - 1\right), \tag{8}$$

where κ is the ratio of specific heat capacities, M_1 is the Mach number in the region 1 in Fig. 3, and β_a is the angle of shock wave a to incoming flow. Analogously, the pressure ratio on the shock wave b is given by

$$\frac{p_4}{p_2} = \frac{\kappa - 1}{\kappa + 1}\left(\frac{2\kappa}{\kappa - 1}M_2^2 \sin^2 \beta_b - 1\right). \tag{9}$$

The ratios of total to static pressures in regions 1 and 2 are given by the isentropic formula

$$\frac{p_{01}}{p_1} = \left(1 + \frac{\kappa - 1}{2}M_1^2\right)^{\kappa/(\kappa-1)} \tag{10}$$

and

$$\frac{p_{02}}{p_2} = \left(1 + \frac{\kappa - 1}{2}M_2^2\right)^{\kappa/(\kappa-1)}. \tag{11}$$

The turning angles of the flow on the shock waves a and b are given by [5]

$$\text{tg}\,\delta_a = \frac{2}{\text{tg}\,\beta_a}\left(\frac{M_1^2 \sin^2 \beta_a - 1}{M_1^2(\kappa + \cos 2\beta_a) + 2}\right) \tag{12}$$

and

$$\text{tg}\,\delta_b = \frac{2}{\text{tg}\,\beta_b}\left(\frac{M_2^2 \sin^2 \beta_b - 1}{M_2^2(\kappa + \cos 2\beta_b) + 2}\right). \tag{13}$$

Thanks to that, the only necessary input data required for the analysis are the incoming Mach numbers and the trailing edge angle, showed in Tab. 4.1.
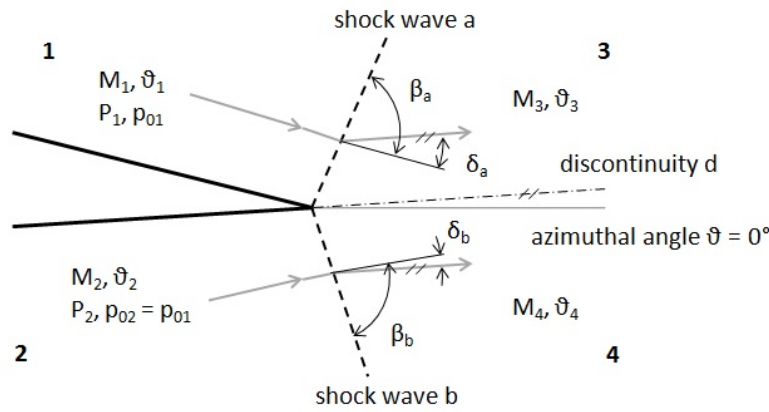
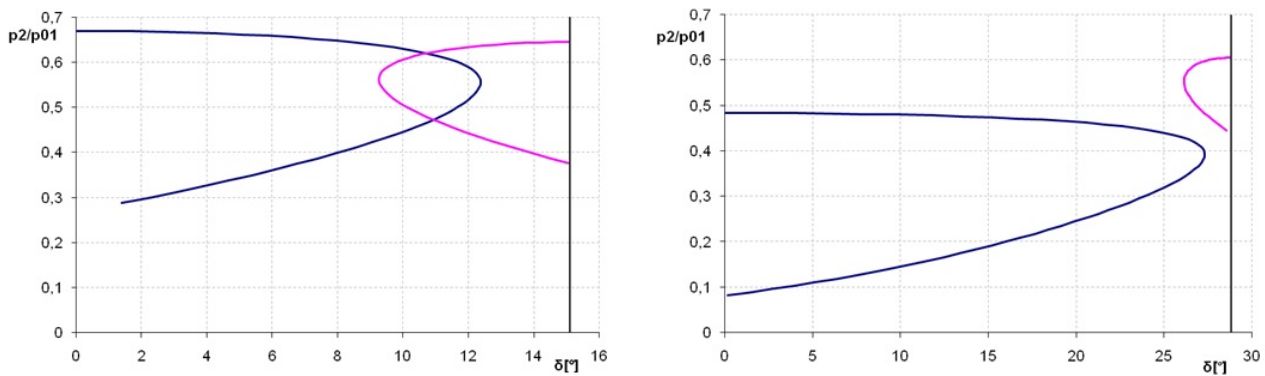FIGURE 6. Trailing edge oblique shocks configuration.

FIGURE 7. Shock polars for both variants: a) Case I, b) Case II.

The azimuthal flow angles ϑ_3 and ϑ_4 can be expressed as follows:

$$\vartheta_3 = \vartheta_1 + \delta_a \qquad (14)$$

and

$$\vartheta_4 = \vartheta_2 - \delta_b. \qquad (15)$$

The trailing edge angle is, of course

$$\delta_{\text{TE}} = \vartheta_2 - \vartheta_1 = \delta_a + \delta_b. \qquad (16)$$

Equations (8), (10) and (12) give the final dependence of static to total pressure ratio p_3/p_{01} on turning angles δ_a for $M_1 = \text{const}$ when

$$\beta_a = \text{var}\Big\langle \arcsin \frac{1}{M_1} < \beta_a < 90° \Big\rangle.$$

The dependence is depicted in the diagrams in Fig. 7 as a blue curve. Equations (9), (11) and (14) give the final dependence of the ratio of static pressure p_4/p_{01} on the turning angles δ_b for $M_2 = \text{const}$ when

$$\beta_b = \text{var}\Big\langle \arcsin \frac{1}{M_2} < \beta_b < 90° \Big\rangle.$$

The dependence is depicted in the diagrams in Fig. 7 as a red curve.

Noting that thanks to the ambiguous character of the supersonic flow, such relations give two values of

the pressure ratio for each possible wave angle which fulfill conditions of (5) and (6) [6] up to the maximum value where the wave detaches and changes to normal shock. The solution with a higher value of p/p_{01} represents an unstable strong shock solution and the solution with lower value of p/p_{01} represents a weak stable solution. The points of intersection define the overall solution of the supersonic flow past the sharp trailing edge. The results of this analysis are the shock polars shown in Figs. 4.2. Every "half-heart-shaped" line represents one side of the profile and the vertical line is the value of the trailing edge angle.

Shock polars for the Case I airfoil configuration, with a solid vertical line representing the trailing edge angle of a value of 15.1°, are depicted in Fig. 7a. Both polars intersect twice and, considering that we are looking for a stable solution, the result is the lower point of intersection. The absolute value of the flow turning angle of the profile is approximately 10.8° on the upper side and 4.3° on the lower side. To compare these numbers with the CFD results, the values from the nearest cell of the shock are approximately 10.9° for the upper side and 4.0 for the lower side. That is a very satisfying result considering the finite character of the computational mesh on one side and the ideal gas dynamics theory on the other.

In Fig. 7b, shock polars for the airfoil of Case II (thicker, more cambered profile and limit variant)
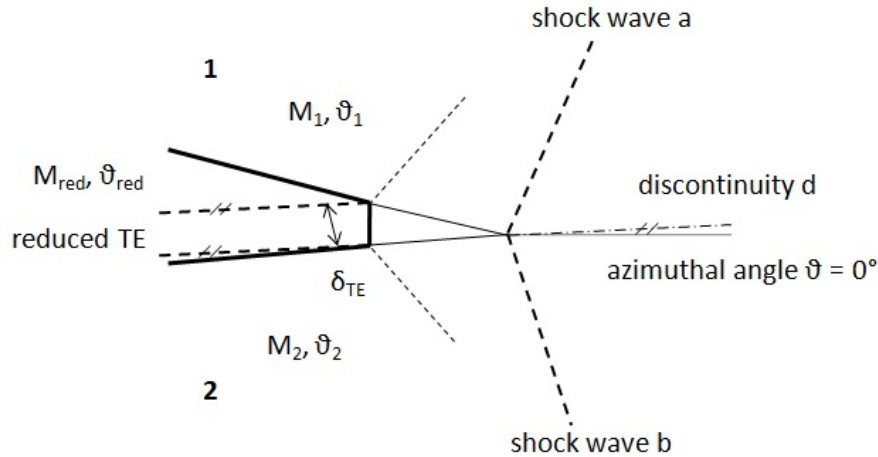
FIGURE 8. Trailing edge configuration with reduced parameters.

with the trailing edge angle 28.8° are shown. The first noticeable difference is the fact that the polars do not intersect, resulting in a questionable irregular solution for this configuration. However, the contour in Fig. 5 above, with no obvious oblique shock on the lower side of the profile, already predicted nonstandard behavior.

5. REDUCED PARAMETER ANALYSIS OF SUPERSONIC FLOW PAST TRAILING EDGE

For a deeper investigation of this problem, the model of nonsymmetrical supersonic flow past a trailing edge [7] is proposed (Fig. 8). The nonsymmetrical supersonic flow past a trailing edge can be reduced to a symmetric case by means of the following relations, in order to obtain some results for an analysis of irregular configuration as well. The reduced value of the azimuthal angle of the flow upstream and downstream (namely azimuthal angle of discontinuity d) of a symmetric trailing edge is given by

$$\vartheta_{\mathrm{red}} = \frac{\vartheta_1 + \upsilon_1 + \vartheta_2 - \upsilon_2}{2} \qquad (17)$$

and the reduced value of Prandtl-Meyer function

$$\upsilon_{\mathrm{red}} = \vartheta_1 + \upsilon_1 - \vartheta_{\mathrm{red}} = \vartheta_{\mathrm{red}} - \vartheta_2 + \upsilon_2, \qquad (18)$$

where the Prandtl-Meyer function is [5]

$$v(M) = -\sqrt{\frac{\kappa+1}{\kappa-1}} \operatorname{arctg} \sqrt{\frac{\kappa+1}{\kappa-1}(M^2-1)}$$
$$+ \operatorname{arctg} \sqrt{M^2-1}. \quad (19)$$

The reduced parameters analysis proved the possibility to apply the model in Fig. 8 also to sharp trailing edges. The application of equations (17) and (18) to Case I of the cusped airfoil proved a regular interaction of supersonic flows on the sharp trailing edge. The reduced value of the azimuthal angle is $\vartheta_{\mathrm{red}} = 10.97°$ and the reduced value of the Prandtl-Meyer function

is $\upsilon_{\mathrm{red}} = 1.23°$. These figures confirm the previous numbers obtained from the basic analysis. For Case II of the cusped airfoil, the reduced value of the azimuthal angle is $\vartheta_{\mathrm{red}} = 30.23°$ and the Prandtl-Meyer function is $\upsilon_{\mathrm{red}} = 3.80°$, while the flow angle obtained from the numerical simulation is approx. 30.8°. That also corresponds well with the reduced angle value. However, further analysis proved the important fact that the condition for the upper branch of exit shock waves $\delta_a \leq \delta_{a,max}$ is not fulfilled. The angle of the shock wave to the incoming flow $\beta_{a,max}$, corresponding to the maximum turning angle $\delta_{a,max}$, is given by the following expression [8]:

$$\beta_{a,max} = \arcsin\left[\frac{1}{\kappa M_1^2}\left(\frac{\kappa+1}{4}M_1^2 - 1\right.\right.$$
$$\left.\left. + \sqrt{(\kappa+1)\left(1 + \frac{\kappa-1}{2}M_1^2 + \frac{\kappa+1}{16}M_1^4\right)}\right)\right]^{1/2}. \quad (20)$$

The interaction of supersonic flows at the trailing edge for Case II is not regular, and the supersonic flow on the upper side of the profile can be separated upstream of the trailing edge [9],or can have an unstable, unsteady character.

6. CONCLUSION

The transonic flow past cusped airfoil profiles was studied, focusing especially on the sharp trailing edge region. Two profiles – Case I and Case II – with known solutions were designed according to modified hodograph methods for potential flow. The flow fields were solved using ANSYS Fluent numerical code for both profile cases. A detailed analysis based on classical gas dynamics proved, for Case I, a good accordance of shock waves parameters at the trailing edge for regular interaction of supersonic flows. Both classical gas dynamics analysis and reduced parameters analysis proved that the transonic flow past Case II resulted in irregular interaction. For Case II a possible separation of flow upstream of the trailing edge, or some unsteady behavior is predicted.

LIST OF SYMBOLS

x x-coordinate [m]

y y-coordinate [m]

ϑ Azimuthal angle [°]

υ Prandtl-Meyer function [°]

M Mach number [–]

T T-coordinate [°]

S S-coordinate [°]

P Camber/thickness parameter [–]

α Angle of attack [°]

τ Thickness to chord ratio [–]

ω Camber to chord ratio [–]

c Chord length [m]

cp Pressure coefficient [–]

p Pressure [Pa]

β Wave angle [°]

δ Turning angle [°]

κ Specific heat capacity ratio [–]

REFERENCES

[1] Jameson, A., Ou, K. *50 years of transonic aircraft design*, Progress in Aerospace Design, Vol.44, Is.5, 2011, pp. 308-318 DOI:10.1016/j.paerosci.2011.01.001

[2] Sobieczky, H. *Tragende Schnabelprofile in Stossfreier Schnallanstormung*, ZAMP 26, 1975 (in German)

[3] Stodulka, J., Sobieczky, H. *On transonic flow models for optimized design and experiment*, European Physical Journal Web of Conferences 67, 2014 DOI:10.1051/epjconf/20146702111

[4] Halama, J. *Transonic flow of wet steam - numerical simulation*, Acta Polytechnica, Vol.52, No.6, 2012

[5] Shapiro, A. H. *The dynamics and thermodynamics of compressible fluid flow*, The Ronald Press Company, New York, 1953

[6] Safarik P. *The flow in the supersonic exit of blade cascades*, Archives of Mechanics, Vol.26, No.3, 1974, pp. 529-533

[7] Safarik, P. *Application of method of characteristics at calculation of flow past blade cascades*, Report of IT CAS No. T-178/75, 1975 (in Czech)

[8] Zucrow, M. J., Hoffman J. D. *Gas dynamics*, John Wiley and Cons, INC, New York, 1976.

[9] Bibin, J., Kulkarni, V.N., Natarajan, G., *Shock wave boundary layer interactions in hypersonic flows*, International Journal of Heat and Mass Transfer, Vol.70, 2014, pp. 81-90 DOI:10.1016/j.ijheatmasstransfer.2013.10.072